JGP Journal of General Physiology

METHODS AND APPROACHES

Null method to estimate the maximal P_A at subsaturating concentrations of agonist

Allison L. Germann[1], Spencer R. Pierce[1], Joe Henry Steinbach[1], and Gustav Akk[1]

The maximal probability of being in an active state ($P_{A,max}$) is a measure of gating efficacy for a given agonist acting on a given receptor channel. In macroscopic electrophysiological recordings, $P_{A,max}$ is typically estimated by comparing the amplitude of the current response to a saturating concentration of a test agonist to that of a reference agonist with known P_A. Here, we describe an approach to estimate the $P_{A,max}$ for low-efficacy agonists at subsaturating concentrations. In this approach, the amplitude of the response to a high-efficacy control agonist applied alone is compared with the amplitude of the response to a control agonist coapplied with the low-efficacy test agonist that binds to the same site(s). If the response to the combination is larger than the response to the control agonist alone, then the $P_{A,max}$ of the test agonist is greater than the P_A of the control response. Conversely, if the response to the control agonist is reduced upon exposure to the test agonist, then the $P_{A,max}$ of the test agonist is smaller than the P_A of the control response. The exact $P_{A,max}$ of the test agonist can be determined by testing its effect at different concentrations of the control agonist to estimate the P_A at which the effect changes direction. The main advantage of this approach lies in the ability to use low, subsaturating concentrations of the test agonist. The model-based predictions are supported by observations from activation of heteromeric and homomeric $GABA_A$ receptors by combinations of high- and low-efficacy orthosteric agonists.

Introduction

Agonist concentration–response relationships provide a variety of fundamental information about the properties and function of a receptor channel in the presence of a given agonist. The level at which the concentration–response relationship saturates can provide insight into the gating efficacy of the agonist. To that end, in macroscopic electrophysiological recordings, the standard, normalized concentration–response relationships are rescaled in units of probability of being in the active state (P_A units). This is done by comparing the amplitudes of peak responses to the test agonist to that of a reference agonist for which the P_A is known. For example, in the case of heteromeric $GABA_A$ receptors, we and others have employed as a reference agonist the combination of saturating GABA and an allosteric agonist, e.g., propofol or etomidate, which is considered to activate all receptors and generate a peak response with P_A of 1 (Feng et al., 2014; Shin et al., 2017). The P_A at which the concentration–response curve for the test agonist saturates is its maximal P_A ($P_{A,max}$).

Estimation of $P_{A,max}$ from a concentration–response curve requires the use of near-saturating concentrations of the test agonist. In practice, that is not optimal in some cases, for example, when there is limited availability of the compound or the compound has additional functional effects that selectively manifest at high concentrations. Here, we describe an approach to estimate $P_{A,max}$ while employing only subsaturating concentrations of the agonist. In this approach, the test agonist is coapplied with a control agonist for which the P_A is known or can be determined. If the P_A of the control response is less than the $P_{A,max}$ of the test agonist, then co-exposure to the test agonist is expected to increase the response to the control agonist. Conversely, coapplication of the test agonist reduces the response to the control agonist if the latter generates a response with a P_A greater than $P_{A,max}$ of the test agonist. Importantly, the direction of the effect does not depend on the concentration of the test agonist, although the magnitude of the effect, and, hence, overall resolution are greater at higher concentrations. A caveat is the requirement that the test and control agonists act through the same binding sites.

Materials and methods

The experiments were conducted on the rat α1β2γ2L wild-type and human β3(Q64R+G127T) mutant $GABA_A$ receptors expressed in *Xenopus laevis* oocytes. The GenBank accession

[1]Department of Anesthesiology, Taylor Family Institute for Innovative Psychiatric Research, Washington University School of Medicine, St. Louis, MO, USA.

Correspondence to Gustav Akk: akk@wustl.edu.

numbers are NM_183326 for α1, NM_012957 for β2, NM_183327 for γ2L, and NM_000814.5 for β3. The β3 mutant clone was purchased from Twist Bioscience. Synthesis of cRNA and details of oocyte handling and injection have been described in detail previously (Shin et al., 2017). The electrophysiological recordings were done using two-electrode voltage clamp at room temperature. The oocytes were voltage-clamped at −60 mV. Bath and agonist-containing solutions were gravity-applied (flow rate: 8 ml/min) from glass syringes through Teflon tubing, and switched manually using a perfusion system containing four-port bulkhead switching valves and medium pressure six-port bulkhead valves (IDEX Health and Science). The bath solution was ND96 (96 mM NaCl, 2 mM KCl, 1.8 mM $CaCl_2$, 1 mM $MgCl_2$, 5 mM HEPES; pH 7.4). Stock solutions of GABA (500 mM), piperidine-4-sulfonic acid (P4S; 3 mM), β-alanine (20 mM), and histamine (100 mM) were made in ND96 and stored at −20°C. Propofol stock solution was made in DMSO at 200 mM and stored at room temperature. Dilutions to final, working concentrations and adjustment of pH when needed were done on the day of the experiment.

The current responses were amplified with an OC-725C (Warner Instruments) or Axoclamp 900A amplifier (Molecular Devices), low-pass filtered at 40 Hz, digitized at 100 Hz with Digidata 1200 or 1320 series digitizers (Molecular Devices), and stored using Clampex (pClamp software package; Molecular Devices). Analyses to estimate current amplitudes were done using Clampfit (pClamp).

Two principal types of electrophysiological recordings were done. The first was measurement of standard concentration–response relationships to estimate the maximal level of activity from saturation of the curve. The second was measurement of the effect of coapplication of a low-efficacy agonist on the response to a high-efficacy agonist.

In P4S concentration–response measurements, oocytes expressing the α1β2γ2L receptor were exposed to 1 µM to 1 mM P4S. The durations of drug applications were 20–40 s, and the individual applications were separated by 2- to 3-min washes in ND96. For normalization purposes, to estimate the P_A of peak responses, each oocyte was additionally exposed to the combination of 1 mM GABA + 50 µM propofol.

To measure the modulatory effects of P4S on α1β2γ2L receptors activated by GABA or β-alanine, the receptors were activated by 20- to 40-s applications of 0.1–10 µM GABA or 0.2–1 mM β-alanine, and their combinations with 10–100 µM P4S. Each oocyte was exposed to a single concentration of GABA or β-alanine, and their combination with P4S. Each oocyte was also tested with 1 mM GABA + 50 µM propofol.

The histamine concentration–response curve for the mutated β3 receptor was measured by exposing oocytes expressing the β3(Q64R+G127T) receptor to 1–50 mM histamine. For normalization, each cell was also exposed to 1 mM GABA + 50 µM propofol. In separate experiments, we measured the ratio of peak responses to 1 mM GABA + 50 µM propofol and 1 mM pentobarbital. Pentobarbital is a highly efficacious agonist of β3 homomeric receptors, considered to activate all receptors and generate a peak P_A of 1 (Eaton et al., 2015). The calculated $P_{A,1\ mM\ GABA\ +\ 50\ \mu M\ propofol}$ was 0.84 ± 0.07 (n = 6). Unlike the wild-type β3 receptor, the β3(Q64R+G127T) receptor is minimally constitutively active ($P_{A,const.}$ = 0.004 ± 0.004; n = 12), and no correction for $P_{A,const.}$ was needed to calculate P_A. The coapplication experiments were done by activating the β3(Q64R+G127T) receptor by 0.2–1 mM GABA in the absence and presence of 1 or 2 mM histamine.

The concentration–response data were fitted with the Hill equation or with Eq. 1 (below). The observations are presented as mean ± SD (number of oocytes). Experimenters were not blinded to experimental conditions, specifically to the drug concentrations employed. The oocytes were chosen randomly.

Results

Theory and simulations

In the co-agonist model (Forman, 2012; Steinbach and Akk, 2019), the P_A in the presence of a single agonist X (Scheme 1, Appendix) is expressed as:

$$P_{A,[X]} = \frac{1}{1 + L\left(\frac{1+[X]/K_X}{1+[X]/(K_X c_X)}\right)^{N_X}} \quad (1)$$

where L (the ratio of resting to active receptors in the absence of an agonist) is a measure of background activity due to constitutive activation of the receptor, K_X is the equilibrium dissociation constant for agonist X in the resting receptor, c_X is the ratio of the equilibrium dissociation constants for X in the active and resting receptor, and N_X is the number of binding sites for X.

At saturating concentrations of X, Eq. 1 reduces to:

$$P_{A,max,X} = \frac{1}{1 + L c_X^{N_X}} \quad (2)$$

In the presence of two agonists, X and Y, that bind to the same N sites (Scheme 2, Appendix), the state equation is:

$$P_{A,[X],[Y]} = \frac{1}{1 + L\left(\frac{1+[X]/K_X+[Y]/K_Y}{1+[X]/(K_X c_X)+[Y]/(K_Y c_Y)}\right)^{N}} \quad (3)$$

where K_Y is the equilibrium dissociation constant for Y in the resting receptor and c_Y is the ratio of the equilibrium dissociation constant for Y in the active receptor to K_Y. Other terms are as defined above.

One prediction made by the coagonist model is that when a high-efficacy agonist (e.g., agonist X) is coapplied with a low-efficacy agonist (agonist Y) that binds to the same N sites, the response to the combination is greater than the response to agonist X alone when $P_{A,[X]} < P_{A,max,Y}$, and, conversely, the coapplication of Y reduces the response to X when $P_{A,[X]} > P_{A,max,Y}$. In other words, there is a "null point" at which the coapplication of Y has no effect on the response to X.

Because X is a higher efficacy agonist than Y, there must be some concentration of X (call it [x′]) for which the P_A equals $P_{A,max,Y}$:

$$P_{A,[x']} = P_{A,max,Y} \quad (4)$$

Substituting in the definitions of $P_{A,[x']}$ and $P_{A,max,Y}$

$$\frac{1}{1+\mathrm{L}\left(\frac{1+[\mathrm{x}']/\mathrm{K_X}}{1+[\mathrm{x}']/(\mathrm{K_X}c_\mathrm{X})}\right)^N}=\frac{1}{1+\mathrm{L}c_\mathrm{Y}{}^N} \tag{5}$$

Rearranging and simplifying the equation results in the following equation:

$$c_\mathrm{Y}{}^N=\left(\frac{1+[\mathrm{x}']/\mathrm{K_X}}{1+[\mathrm{x}']/(\mathrm{K_X}c_\mathrm{X})}\right)^N \tag{6}$$

Taking the *N*th root on both sides and rearranging yields the following expression for [x′]:

$$[\mathrm{x}']=\frac{\mathrm{K_X}c_\mathrm{X}(c_\mathrm{Y}-1)}{(c_\mathrm{X}-c_\mathrm{Y})} \tag{7}$$

Note that the expression does not depend on [Y], so any concentration of Y can be used.

The second step is to determine the concentration of X (call it [x*]) at which the coapplication of Y does not affect the response. That is,

$$\frac{1}{1+\mathrm{L}\left(\frac{1+[\mathrm{x}^*]/\mathrm{K_X}+[\mathrm{Y}]/\mathrm{K_Y}}{1+[\mathrm{x}^*]/(\mathrm{K_X}c_\mathrm{X})+[\mathrm{Y}]/(\mathrm{K_Y}c_\mathrm{Y})}\right)^N}=\frac{1}{1+\mathrm{L}\left(\frac{1+[\mathrm{x}^*]/\mathrm{K_X}}{1+[\mathrm{x}^*]/(\mathrm{K_X}c_\mathrm{X})}\right)^N} \tag{8}$$

Rearranging and simplifying the equation results in the following equation:

$$\left(\frac{1+[\mathrm{x}^*]/\mathrm{K_X}}{1+[\mathrm{x}^*]/(\mathrm{K_X}c_\mathrm{X})}\right)^N=\left(\frac{1+[\mathrm{x}^*]/\mathrm{K_X}+[\mathrm{Y}]/\mathrm{K_Y}}{1+[\mathrm{x}^*]/(\mathrm{K_X}c_\mathrm{X})+[\mathrm{Y}]/(\mathrm{K_Y}c_\mathrm{Y})}\right)^N \tag{9}$$

Taking the *N*th root on both sides and rearranging yields:

$$\left(1+\frac{[\mathrm{x}^*]}{\mathrm{K_X}}\right)\left(1+\frac{[\mathrm{x}^*]}{\mathrm{K_X}c_\mathrm{X}}+\frac{[\mathrm{Y}]}{\mathrm{K_Y}c_\mathrm{Y}}\right)=\left(1+\frac{[\mathrm{x}^*]}{\mathrm{K_X}}+\frac{[\mathrm{Y}]}{\mathrm{K_Y}}\right)\left(1+\frac{[\mathrm{x}^*]}{\mathrm{K_X}c_\mathrm{X}}\right) \tag{10}$$

Expanding the products gives:

$$\left(1+\frac{[\mathrm{x}^*]}{\mathrm{K_X}}\right)\left(1+\frac{[\mathrm{x}^*]}{\mathrm{K_X}c_\mathrm{X}}\right)+\left(1+\frac{[\mathrm{x}^*]}{\mathrm{K_X}}\right)\left(\frac{[\mathrm{Y}]}{\mathrm{K_Y}c_\mathrm{Y}}\right)=\left(1+\frac{[\mathrm{x}^*]}{\mathrm{K_X}c_\mathrm{X}}\right)\left(1+\frac{[\mathrm{x}^*]}{\mathrm{K_X}}\right)+\left(1+\frac{[\mathrm{x}^*]}{\mathrm{K_X}c_\mathrm{X}}\right)\left(\frac{[\mathrm{Y}]}{\mathrm{K_Y}}\right) \tag{11}$$

Simplifying the equation yields:

$$\frac{[\mathrm{x}^*]}{\mathrm{K_X}c_\mathrm{Y}}+\frac{1}{c_\mathrm{Y}}=1+\frac{[\mathrm{x}^*]}{\mathrm{K_X}c_\mathrm{X}} \tag{12}$$

and rearranging gives:

$$\frac{[\mathrm{x}^*]}{\mathrm{K_X}}\left(\frac{1}{c_\mathrm{Y}}-\frac{1}{c_\mathrm{X}}\right)=1-\frac{1}{c_\mathrm{Y}} \tag{13}$$

Multiplying both sides of the equation by $c_\mathrm{X}c_\mathrm{Y}$ and rearranging gives an expression for [x*]:

$$[\mathrm{x}^*]=\frac{\mathrm{K_X}c_\mathrm{X}(c_\mathrm{Y}-1)}{(c_\mathrm{X}-c_\mathrm{Y})} \tag{14}$$

This result (Eqs. 14 and 7) shows that [x*] = [x′], and so the concentration of X at which the coapplication of any concentration of Y has no effect on the magnitude of the response also is the concentration of X that produces a response equal to $\mathrm{P_{A,max,Y}}$.

This is illustrated in Fig. 1, A–C. Agonist X is the high-efficacy agonist with c_X = 0.004 ($\mathrm{P_{A,max,X}}$ = 0.89) and agonist Y is the low-efficacy agonist with c_Y = 0.02 ($\mathrm{P_{A,max,Y}}$ = 0.24). The concentration–response curve for X is right-shifted in the presence of Y (Fig. 1 A). Coapplication of Y enhances the response to low concentrations of X; accordingly, the response ratios (RR, calculated as $\mathrm{I_{X+Y}/I_X}$) are >1 (Fig. 1 B). As the concentration of X is increased the RR are reduced, dropping below 1 due to inhibition of the response to high-efficacy agonist X by the low-efficacy agonist Y. The RR increases at very high [X], approaching 1 when X outcompetes Y for binding. RR plotted against $\mathrm{P_A}$ of the control response (Fig. 1 C) cross the RR = 1 line at $\mathrm{P_{A,X}}$ = $\mathrm{P_{A,max,Y}}$. The value of the intercept can be estimated from linear regression fitting of the RR versus $\mathrm{P_{A,X}}$ relationship, although, due to the concave shape of the relationship the fitted $\mathrm{P_{A,max,Y}}$ is more accurate when using a narrow band of data points near the RR = 1 line.

Experimental validation using heteromeric α1β2γ2L and homomeric β3 $\mathrm{GABA_A}$ receptors

For experimental validation, we first examined the activation of the α1β2γ2L $\mathrm{GABA_A}$ receptor by the high-efficacy agonists GABA and the low-efficacy agonist P4S (Thompson et al., 1999; O'Shea et al., 2000; Steinbach and Akk, 2001; Mortensen et al., 2002). The compounds activate the $\mathrm{GABA_A}$ receptor through interactions with the orthosteric binding sites (Krogsgaard-Larsen et al., 1980; Jones et al., 1998; Akk et al., 2011). We began by conducting P4S concentration–response measurements to estimate the $\mathrm{P_{A,max,P4S}}$ using a conventional approach. The oocytes were exposed to brief applications of 1 µM to 1 mM P4S. For normalization purposes, each oocyte was also exposed to 1 mM GABA + 50 µM propofol, which was assumed to generate a peak response with $\mathrm{P_A}$ of 1 (Shin et al., 2017). Sample current traces are given in Fig. 2 A. Fitting the concentration–response data with the Hill equation gave an $\mathrm{EC_{50}}$ of 33 ± 12 µM (n = 5) and a Hill coefficient of 1.01 ± 0.27. The fitted maximal $\mathrm{P_A}$ was 0.18 ± 0.10. With L constrained to 8,000 (Shin et al., 2017) and N = 2, fitting Eq. 1 to the $\mathrm{P_A}$ data yielded a $\mathrm{K_{P4S}}$ of 14 ± 5 µM and a c_P4S of 0.027 ± 0.009 (Fig. 2 A). The $\mathrm{P_{A,max}}$, $\mathrm{K_{P4S}}$, and c_P4S estimates are similar to those reported previously for the concatemeric α1β2γ2L receptor (Shin et al., 2019).

We then measured the modulation of GABA responses by P4S. Each oocyte was exposed to a brief application of 0.1–10 µM GABA, GABA + P4S, and, for normalization, exposed to 1 mM GABA + 50 µM propofol. The concentration of P4S was held at 10, 30, or 100 µM. P4S increased the responses to low concentrations of GABA and inhibited the responses to high concentrations of GABA. We calculated the RR as $\mathrm{I_{peak,GABA+P4S}/I_{peak,GABA,}}$ and the $\mathrm{P_A}$ of the response to GABA as $\mathrm{I_{peak,GABA}/I_{peak,GABA+propofol}}$. Sample current responses and the log-log relationships between the RR and $\mathrm{P_{A,GABA}}$ are given in Fig. 2 B. Fitting the RR-$\mathrm{P_{A,GABA}}$ data with $y = x^{slope} \times 10^{intercept}$ gave a y = 1 intercept, i.e., the estimated $\mathrm{P_{A,max,P4S}}$, of 0.18 ± 0.05 (data from 21 oocytes) in the presence of 10 µM P4S, 0.18 ± 0.08 (n = 17) in the presence of 30 µM P4S, and 0.23 ± 0.08 (n = 20) in the presence of 100 µM P4S. These $\mathrm{P_{A,max,P4S}}$ estimates are similar to the one obtained from fitting the concentration–response curve (0.18 ± 0.10) despite using P4S at up to 100 times lower concentrations.

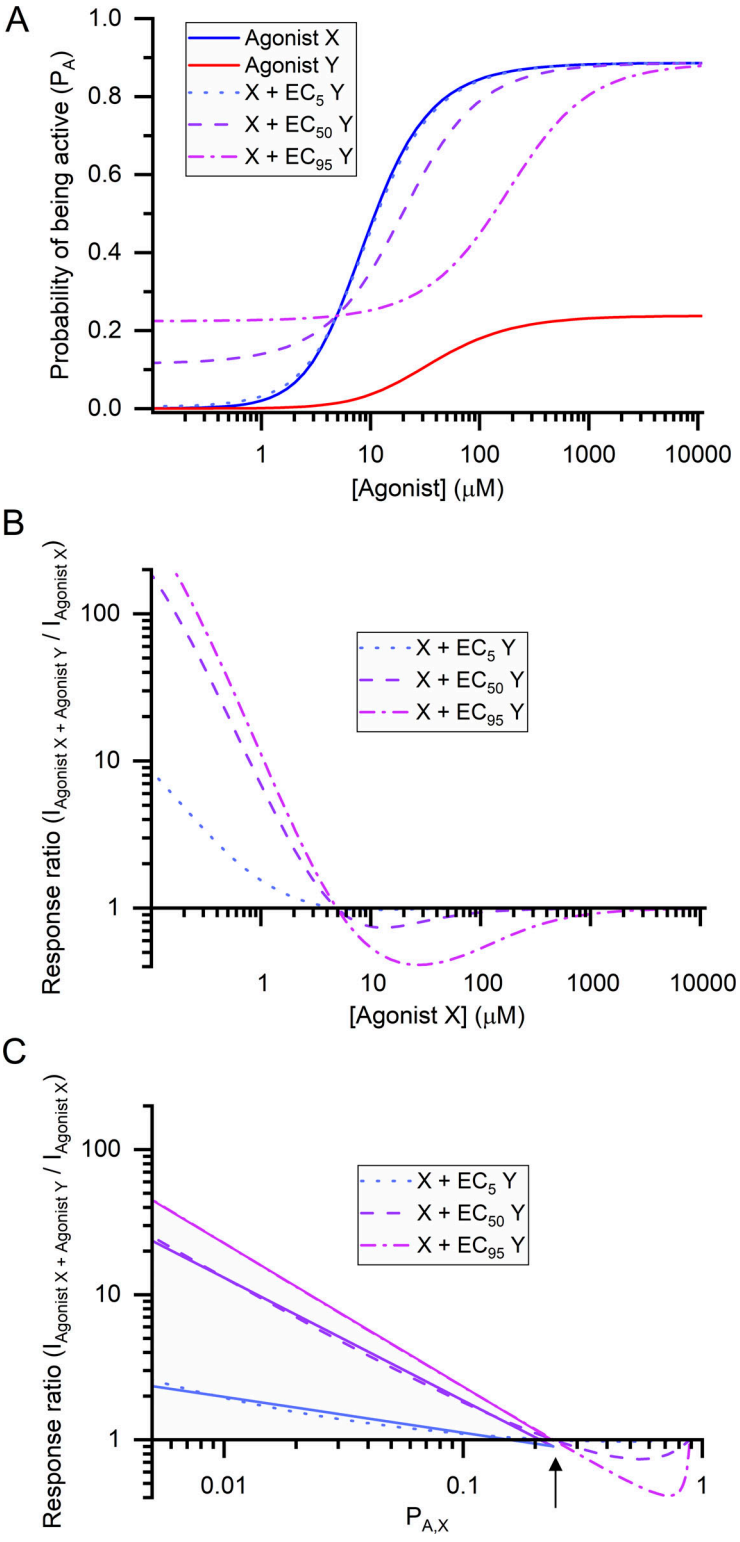

Figure 1. **Predictions of the effects of agonists with differing efficacies. (A)** Concentration–response curves calculated using Eq. 1 for the high-efficacy agonist X (K_X = 20 μM, c_X = 0.004, N_X = 2) and the low-efficacy agonist Y (K_Y = 20 μM, c_Y = 0.02, N_Y = 2). The curves show calculated P_A in the presence of X or Y applied alone (solid blue and red lines, respectively) or X applied in the presence of 2 μM (EC_5), 35 μM (EC_{50}), or 500 μM (EC_{95}) agonist Y (dotted, dashed, or dash-dotted lines, respectively). **(B)** Response ratios (RR), calculated as a response to X + Y over the response to X alone, as a function of the concentration of agonist X. At low concentrations of X, coapplication of Y increases the current response, manifesting as RR > 1. Coapplication of the low-efficacy agonist Y reduces the response to intermediate concentrations of X (RR < 1). RR approaches 1 at high concentrations of X where the latter outcompetes Y. **(C)** Response ratios as a function of the P_A of the response to X. In the co-agonist model (Appendix), the coapplication of Y has no effect on the response to X (i.e., RR = 1) when $P_{A,X} = P_{A,max,Y}$. The calculations for three concentrations of Y (EC_5, EC_{50}, and EC_{95}) indicate different slopes but identical RR = 1 intercepts. The solid lines show linear fits to RR > 1 values. The fits are improved (lower residual sums of squares) at higher concentrations of Y. Note, that the value of $P_{A,max,Y}$ from the high-concentration asymptote for the red line in panel A is identical to the value of the intercept in panel C (shown with arrow).

Next, we examined P4S-mediated effects on responses to the low-affinity, high-efficacy orthosteric agonist β-alanine. The α1β2γ2L $GABA_A$ receptors were activated by 0.2–1 mM β-alanine in the absence and presence of 30 μM P4S. Coapplication of P4S affected the responses to β-alanine, similar to that observed with GABA as a control agonist. The data are summarized in Fig. 2 C. Fitting the RR-$P_{A,β\text{-alanine}}$ data yielded a $P_{A,max,P4S}$ of 0.24 ± 0.08 (n = 20). This is similar to the $P_{A,max,P4S}$ estimates provided above.

Lastly, we measured the ability of histamine to affect GABA-elicited responses in the β3(Q64R+G127T) homomeric mutant receptor. The β3 receptor is normally efficiently activated by histamine but not by GABA due to unfavorable interactions of GABA with key residues in the orthosteric binding site (Saras

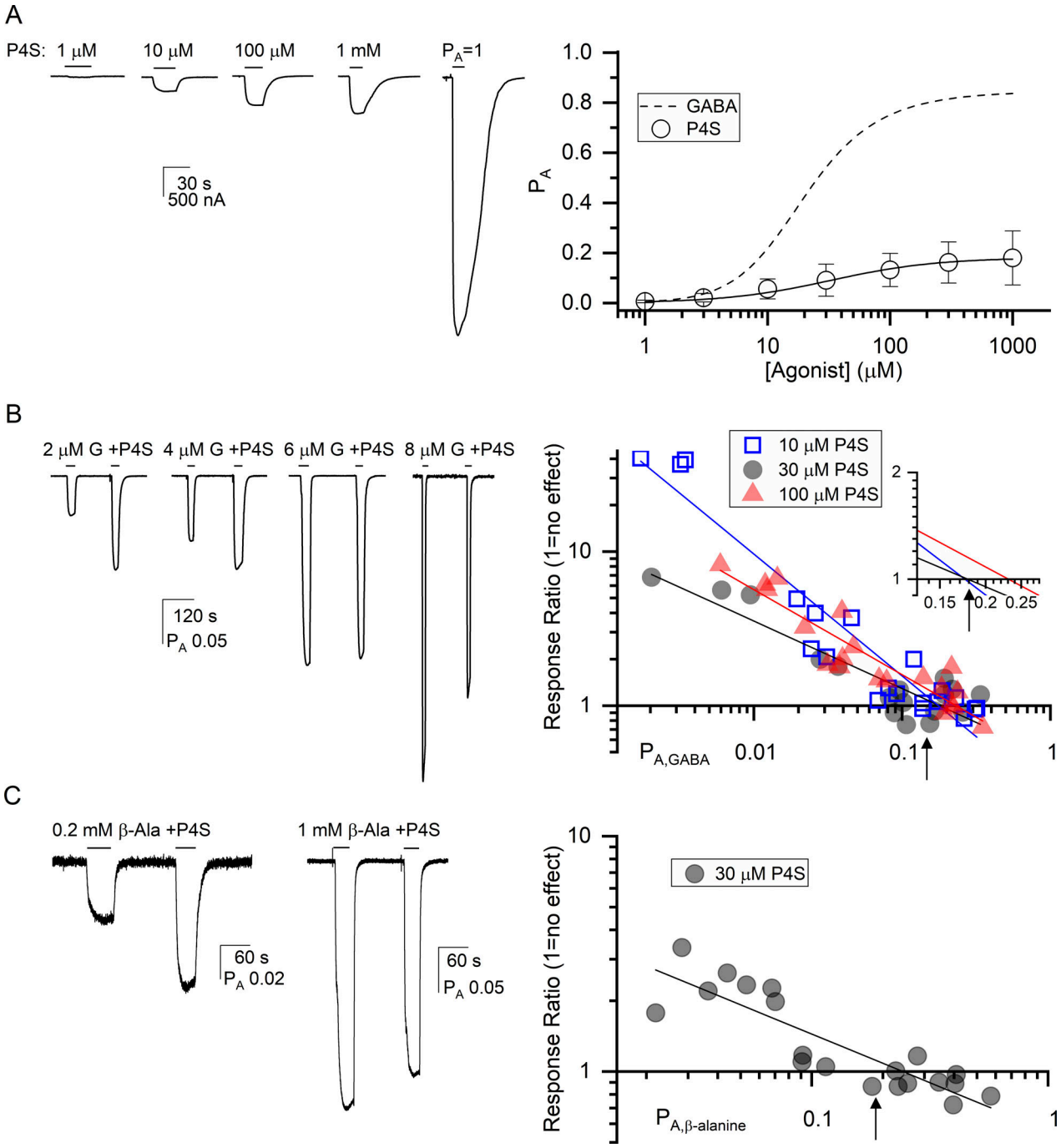

Figure 2. **The effects of P4S on responses to GABA and β-alanine in the a1β2γ2L receptor. (A)** Sample current responses to various concentrations of P4S and the combination of 1 mM GABA + 50 μM propofol (P_A = 1). All traces are from the same cell. The P_A of the peak responses to P4S was calculated through normalization to the response to 1 mM GABA + 50 μM propofol. The plot shows the concentration–response relationships for GABA and P4S. The data points give means ± SD from five cells. The solid line was calculated using the averaged fitting results (EC_{50} = 33 μM, n_{Hill} = 1.01, and Y_{max} = 0.18). The dashed line gives the P_A curve in the presence of GABA reported previously for the α1β2γ2L receptor (Shin et al., 2017). **(B)** Sample current responses to 2–8 μM GABA in the absence and presence of 100 μM P4S. The coapplication of P4S potentiates low-GABA currents and inhibits high-GABA currents. The P_A of the control responses were 0.047 (2 μM GABA), 0.079 (4 μM GABA), 0.22 (6 μM GABA), and 0.35 (8 μM GABA). The plot gives the response ratios as a function of $P_{A,GABA}$. The experiments were done in the presence of 10, 30, or 100 μM P4S. The lines show linear fits to RR > 1 values. The fitted RR = 1 intercepts are 0.18 ± 0.05 (10 μM P4S), 0.18 ± 0.08 (30 μM P4S), and 0.23 ± 0.08 (100 μM P4S). The inset shows the RR = 1 intercepts at higher resolution. **(C)** Sample current responses to 0.2 and 1 mM β-alanine (β-Ala) in the absence and presence of 30 μM P4S. Coapplication of P4S potentiates low-β-alanine currents and inhibits high-β-alanine currents. The P_A of the control responses were 0.036 (0.2 mM β-alanine) and 0.18 (1 mM β-alanine). The plot gives the response ratios as a function of $P_{A,β\text{-alanine}}$. The line shows linear fit with the RR = 1 intercept at 0.24 ± 0.08. The arrows in panels B and C indicate the value of $P_{A,max}$ (0.18) for P4S estimated from the high-concentration asymptote of the concentration–response curve in panel A.

et al., 2008; Masiulis et al., 2019; Sente et al., 2022). The Q64R+G127T mutations at the complementary side of the binding interface restore sensitivity to GABA, albeit at the expense of sensitivity to histamine (Gottschald Chiodi et al., 2019). For an initial independent estimate of gating efficacy in the presence of histamine, we measured the histamine concentration–response relationship. Oocytes expressing the β3(Q64R+G127T) receptor were exposed to 1–50 mM histamine, and, for normalization, to 1 mM GABA + 50 µM propofol. Fitting the concentration–response curve yielded a $P_{A,max,histamine}$ of 0.50 ± 0.09 (n = 6). The EC_{50} of the curve was at 9.0 ± 0.5 mM and the Hill coefficient was 1.45 ± 0.16 (Fig. 3 A). To test the null method, we measured the effects of 1 and 2 mM histamine on responses generated by 0.2–1 mM GABA. The extent and direction of effects scaled with $P_{A,GABA}$ (Fig. 3 B). Fitting the RR-$P_{A,GABA}$ data yielded a $P_{A,max,histamine}$ of 0.33 ± 0.04 (n = 8) in the presence of 1 mM histamine, and 0.51 ± 0.12 (n = 15) in the presence of 2 mM histamine.

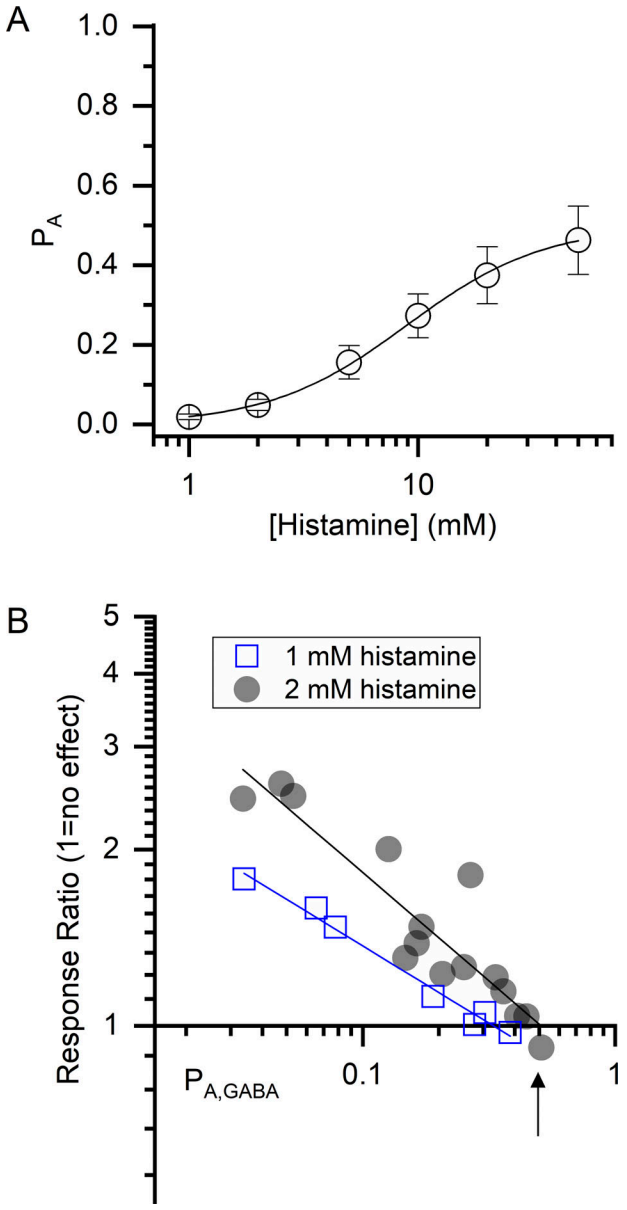

Figure 3. **The effects of histamine on responses to GABA in the β3(Q64R+G127T) receptor. (A)** Concentration–response relationship for histamine. The data points give means ± SD from six cells. The solid line was calculated using the averaged fitting results (EC_{50} = 9 mM, n_{Hill} = 1.45, and Y_{max} = 0.50). **(B)** Response ratios as a function of $P_{A,GABA}$. The experiments were done in the presence of 1 or 2 mM histamine. The lines show linear fits with the RR = 1 intercept at 0.33 ± 0.04 at 1 mM histamine and 0.51 ± 0.12 at 2 mM histamine. The arrow in panel B indicates the value of $P_{A,max}$ (0.50) for histamine estimated from the high-concentration asymptote in panel A.

Discussion

Here, we have described an approach to estimate $P_{A,max}$ for low-efficacy agonists. The approach entails measurement of the effect of coapplication of a low-efficacy test agonist on the response to a high-efficacy control agonist and estimation of the P_A of the control agonist at which coapplication of the low-efficacy agonist has no effect on current amplitude. Model-based predictions were experimentally validated on heteromeric and homomeric $GABA_A$ receptors using combinations of orthosteric agonists. The major benefit of the approach lies in the ability to employ low, subsaturating concentrations of the test agonist while the conventional approach to estimate $P_{A,max}$ in macroscopic recordings through fitting the concentration–response relationship requires the use of near-saturating concentrations of agonist. Specifically, in our validation experiments, similar $P_{A,max}$ values for P4S or histamine were obtained conventionally by fitting the concentration–response curves and the null method employing the low-efficacy agonists at up to 100 times less than a saturating concentration.

Colquhoun (1973) published a figure similar to our Fig. 1 A (his Fig. 7 c) and noted in the legend that the P_A at the point where the lines cross (i.e., the concentration of the higher efficacy agonist for which the coapplication of the lower efficacy agonist has no effect) is equal to the $P_{A,max}$ for the lower efficacy agonist. However, the result is presented without derivation, and to the best of our knowledge was not tested experimentally. Steinbach and Akk (2019) also published a similar figure (their Fig. 4 B) and reported that the concentration of the higher efficacy agonist was given by the relationship in our Eq. 7. However, the result is again presented without derivation, and the P_A at that point is not given. Accordingly, elements of our approach were known but had not been fully developed and utilized in experimental work.

As noted above, the null method described here requires that the two agonists bind to the same sites. The combination of two agonists interacting with distinct sites results in allosteric potentiation. For example, coapplication of the low-efficacy allosteric agonist neurosteroid allopregnanolone with the orthosteric agonist GABA results in potentiation despite the $P_{A,max,allopregnanolone}$ being very low (0.002; Shin et al., 2019).

While the approach is valid at any concentration of test agonist, the simulations shown in Fig. 1 C indicate that the slope of the RR versus P_A line becomes smaller as the concentration of test agonist is reduced. This is confirmed by observations summarized in Figs. 2 and 3. A smaller slope can reduce precision in real-life experiments, as evident, for example, when

comparing modulation of GABA-activated receptors by 1 versus 2 mM histamine (Fig. 3 B). We also note that in our experiments, we estimated the P_A of the control response to GABA or β-alanine through normalization to the peak response to the combination of 1 mM GABA + 50 µM propofol in the same cell. While it is possible to base the $P_{A,control}$ on previously reported activation properties of the control agonist, it is likely more accurate when comparing it to the reference response in the same cell.

We note that the approach utilizes pseudo steady-state peak responses. This can lead to inaccuracies if the amplitude of the peak is curtailed by rapid development of desensitization or block. In the case of these $GABA_A$ receptors expressed in *Xenopus* oocytes, desensitization is relatively slow (c.f. the traces in Fig. 2) and the estimate of $P_{A,max}$ for the agonist GABA (~0.8) is similar in whole-oocyte responses (Feng et al., 2014; Shin et al., 2017) and single-channel clusters (Steinbach and Akk, 2001; Lema and Auerbach, 2006). A second concern is that the two compounds being applied need to have similar kinetics for their responses so that both effects will be at a pseudo steady-state at the peak. If these criteria are not met, the approach will not provide an accurate estimate.

$P_{A,max}$ estimates can be directly obtained in single-channel recordings through measurements of intracluster P_A or kinetic properties of bursts of openings (e.g., Sine and Steinbach, 1986; Zhang et al., 1995; Steinbach and Akk, 2001). The potential drawbacks associated with these approaches, however, are low single-channel conductance in some receptor channels (e.g., sub-pS for homomeric ρ $GABA_A$ and 5-HT_{3A} receptors [Brown et al., 1998; Wotring et al., 1999]) or that activity originating from a single ion channel cannot be reliably identified due to low efficacy of the agonist (e.g., many quaternary ammonium derivatives on the nicotinic receptor [Zhou et al., 1999; Akk and Steinbach, 2003]). An additional approach to measure $P_{A,max}$ in macroscopic recordings is non-stationary noise analysis, but this method is best suited for $P_{A,max}$ values of 0.5 and greater, and it also requires the use of saturating concentrations of agonist (Sigworth, 1980; Lingle, 2006). The null method described here is suitable for a nearly unlimited range of P_A values and, as we have shown, can produce independently verified $P_{A,max}$ estimates at low concentrations of the low-efficacy agonist.

Our studies were conducted on the $GABA_A$ receptor, which is well-characterized and has a rich pharmacology enabling the selection of agonists appropriate for the present study. There is at least qualitative published evidence that the model holds for related receptor channels. In the muscle-type nicotinic receptor, some non-depolarizing neuromuscular blocking agents potentiate the current response to low concentrations of acetylcholine and inhibit the response to high concentrations of acetylcholine (Steinbach and Chen, 1995; Fletcher and Steinbach, 1996). In the neuronal-type α4β4 nicotinic receptor, the low-efficacy orthosteric agonist choline enhances responses to low concentrations of acetylcholine and nicotine while reducing responses to high concentrations of acetylcholine (Zwart and Vijverberg, 2000).

In sum, we have presented an electrophysiological approach to estimate maximal P_A at low, subsaturating concentrations of a test agonist. Experimental validation was performed on heteromeric α1β2γ2L and homomeric β3 $GABA_A$ receptors activated by several combinations of orthosteric agonists, demonstrating quantitative agreement between estimates of $P_{A,max}$ from a traditional approach and the novel null method.

Appendix

Kinetic schemes and equations

One ligand

The two-state concerted-transition model was first proposed by Monod and coworkers (Monod et al., 1965). It was initially applied to transmitter-gated channels by Karlin (1967) and has subsequently been extensively used in studies of the $GABA_A$ receptor (e.g., Chang and Weiss, 1999; Forman, 2012; Germann et al., 2019b). It is a remarkably simple model, originally formulated in terms of a homomultimeric protein with N subunits, although it has usually been implemented for proteins with N sites. The protein can exist in two states (Resting and Active), and all subunits (sites) undergo the state transition at the same time—there is never a mixture of R- and A-state subunits in a protein. In the absence of any agonist or antagonist, the ratio of R to A states is given by the parameter L. The value of L is typically high, reflecting a low level of constitutive activity (Shin et al., 2017). A chemical (X) binds to the R state with dissociation constant $K_{R,X}$ and to the A state with $K_{A,X} = c_X K_{R,X}$. Again, an essential feature of the model is that all subunits (sites) have the same affinity for X, either $K_{R,X}$ or $K_{A,X}$. A more complete discussion of the points presented here is in Steinbach and Akk (2019).

A reaction scheme for the case that $N = 3$ is shown as Scheme 1:

$$\begin{array}{ccccccc} \mathbf{A} & \rightleftharpoons & \mathbf{XA} & \rightleftharpoons & \mathbf{X_2A} & \rightleftharpoons & \mathbf{X_3A} \\ \Updownarrow & & \Updownarrow & & \Updownarrow & & \Updownarrow \\ \mathbf{R} & \rightleftharpoons & \mathbf{XR} & \rightleftharpoons & \mathbf{X_2R} & \rightleftharpoons & \mathbf{X_3R} \end{array}$$

Scheme 1.

As given in the Theory and simulations section, the probability of being active in the presence of X is:

$$P_{A,[X]} = \frac{1}{1 + L\left(\frac{1+[X]/K_X}{1+[X]/(K_X c_X)}\right)^{N_X}}$$

where $K_X = K_{R,X}$, [X] is the concentration of X, $c_X = K_{A,X}/K_{R,X}$, and other terms are as defined above. X is an agonist if $K_{A,X}$ is less than $K_{R,X}$ ($c_X < 1$) and so stabilizes the active state.

A great advantage of the model is that only four parameters are needed to describe the effect of X: one describes a property of the receptor (L), which reflects the energy difference between the R and A states in the absence of agonist. Three describe properties of the chemical: N_X (the number of sites), $K_{R,X}$ (the affinity for the resting state), and $K_{A,X}$ (the affinity for the active state). Scheme 1 can be lengthened to any number of sites and the same equation is applicable with the appropriate N value.

The model can be directly applied to the case in which X binds to two separate and distinct classes of sites, say site I and site II. In this case, two terms (one for each class) multiply to reflect the stabilization of the A state through the two classes of sites:

$$P_{A,[X]} = \frac{1}{1 + L\left(\frac{1+[X]/K_{I,X}}{1+[X]/(K_{I,X}c_{I,X})}\right)^{N_{I,X}}\left(\frac{1+[X]/K_{II,X}}{1+[X]/(K_{II,X}c_{II,X})}\right)^{N_{II,X}}}$$

Two ligands

When two chemicals act on the receptor, they fall into two general classes: they share binding sites or they bind to separate sites. (Of course, there can be some embellishments; for example, they could share some but not all sites.) For the application of the null method, the two chemicals must share sites and each must interact with all of the sites. If the chemicals bind to distinct sites, the form of the equation for the probability of being active is essentially identical to the case when one drug binds to two distinct classes of sites:

$$P_{A,[X],[Y]} = \frac{1}{1 + L\left(\frac{1+[X]/K_X}{1+[X]/(K_X c_X)}\right)^{N_X}\left(\frac{1+[Y]/K_Y}{1+[Y]/(K_Y c_Y)}\right)^{N_Y}}$$

where [Y] is the concentration of Y and $K_Y = K_{R,Y}$. This equation was first presented by Rubin and Changeux (1966). It illustrates another advantage of this simple model: the interaction of two chemicals that bind to distinct sites can be fully characterized by the actions of the chemicals independently. All interactions are mediated by altering the distribution of the population of receptors between the R and A states, with no other effects on affinities. We will not discuss this case further.

When X and Y bind to the same sites there is then competition for occupancy. Scheme 2 shows a receptor with three sites that can be occupied by X or Y.

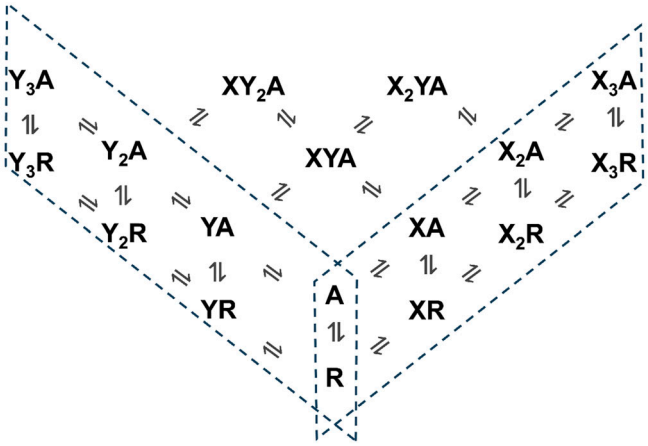

Scheme 2.

Here, active (A) states are on the upper plane, and resting (R) states are on the lower. The two sides show the Scheme 1 scheme for X (right side) and Y (left side), indicated by the dashed boxes. The cases when both chemicals are bound are shown in between the individual Scheme 1 sides. Note that cases when resting receptors have bound both chemicals are obscured (XYR, XY_2R, and X_2YR).

As given in the Theory and simulations section, the probability of being active in the presence of the chemicals X and Y is:

$$P_{A,[X],[Y]} = \frac{1}{1 + L\left(\frac{1+[X]/K_X+[Y]/K_Y}{1+[X]/(K_X c_X)+[Y]/(K_Y c_Y)}\right)^{N}}$$

where the terms are as defined earlier. Scheme 2 can be altered to increase the number of identical sites, and the equation will be applicable with the appropriate *N* value. Karlin (1967) was the first to derive this equation. Again, the interaction between X and Y can be fully described by the parameters derived from studies of the actions of X or Y acting alone. The number of available forms of ligated receptors is reduced by the competition between X and Y.

Application of the concerted transition model to transmitter-gated membrane channels

Karlin (1967) first proposed that the MWC model could be used to analyze macroscopic responses of nicotinic acetylcholine receptors, although the analysis presented was limited. Subsequently, several studies have used the model in studies of, for example, cyclic nucleotide-gated channels (Goulding et al., 1994) or TRPV1 receptors (Li and Zheng, 2024).

It has been most extensively studied for the muscle-type nicotinic receptor and the $GABA_A$ receptor. Analysis of nicotinic receptor activation has focused on single-channel currents, and it was found that the individual rate constants can be well described by an MWC model (Auerbach, 2012). The study of $GABA_A$ receptors was initiated by an analysis of the activation of a series of gain-of-function mutations and demonstrated a critical aspect of the model—that receptors could be active in the absence of an agonist (Chang and Weiss, 1999). Subsequently, S.A. Forman and our own laboratory have extensively analyzed interactions among drugs acting on the receptor. The initial report used interactions of the allosteric agonist etomidate with the orthosteric agonist (GABA) to quantitatively test the applicability of the MWC model (Rüsch et al., 2004). This work emphasized the observation that in the MWC model interactions among ligands can be analyzed using parameters obtained from single-compound experiments because the interactions are mediated through changes in the distribution of the receptor among states rather than specific interactions between agonists (for example on affinities or efficacies). The Forman group has continued work, extending to additional drugs and analysis of mutations (Ruesch et al., 2012; Szabo et al., 2019). The Akk laboratory has extended the work to multiple drug interactions and an increase in the number of states (Cao et al., 2018; Germann et al., 2019a).

Is the concerted transition model realistic?

It is clear that a simple two-state model cannot capture all the information from single-channel studies of multiple open states based on duration or conductance and multiple closed states of different mean durations. Indeed, early studies of nicotinic receptors in *Torpedo* electroplax (Sheridan and Lester, 1977)

demonstrated that activation kinetics did not conform to the predictions for the MWC model (Colquhoun and Hawkes, 1977). More recent work has also found that some interactions among drugs are not fully consistent with the restrictions of the MWC model that all interactions occur through alterations of the distribution of the population of receptors between the R and A states (Szabo et al., 2019) and that the stabilization energy provided by a drug may not be constant for all levels of basal activity (Goldschen-Ohm et al., 2014; Pierce et al., 2024).

However, the model provides an accessible framework for analysis of receptor activation and, in particular, drug interactions. The basic utility and validity of the approach have been supported in studies, especially of $GABA_A$ receptors, and predictions of the model (for instance the present manuscript) have led to some novel insights.

Data availability

The data underlying Figs. 2 and 3 are available in the published article.

Acknowledgments

Eduardo Ríos served as editor.

We thank Professor Andrew Plested for helpful comments during the review of this manuscript.

This study was supported by the National Institutes of Health National Institute of General Medical Sciences grant R35GM140947 and funds from the Taylor Family Institute for Innovative Psychiatric Research.

Author contributions: A.L. Germann: Conceptualization, Data curation, Formal analysis, Investigation, Methodology, Validation, Visualization, Writing - review & editing, S.R. Pierce: Data curation, Formal analysis, Investigation, J.H. Steinbach: Conceptualization, Formal analysis, Methodology, Writing - original draft, Writing - review & editing, G. Akk: Conceptualization, Data curation, Formal analysis, Funding acquisition, Methodology, Project administration, Supervision, Visualization, Writing - original draft.

Disclosures: G. Akk reported that the work was supported by a grant from National Institutes of Health National Institute of General Medical Sciences (R35GM140947) and funds from the Taylor Family Institute for Innovative Psychiatric Research at Washington University in St Louis. No other disclosures were reported.

Submitted: 16 July 2024
Revised: 10 October 2024
Accepted: 7 November 2024

References

Akk, G., P. Li, J. Bracamontes, M. Wang, and J.H. Steinbach. 2011. Pharmacology of structural changes at the GABA(A) receptor transmitter binding site. *Br. J. Pharmacol.* 162:840–850. https://doi.org/10.1111/j.1476-5381.2010.01083.x

Akk, G., and J.H. Steinbach. 2003. Activation and block of mouse muscle-type nicotinic receptors by tetraethylammonium. *J. Physiol.* 551:155–168. https://doi.org/10.1113/jphysiol.2003.043885

Auerbach, A. 2012. Thinking in cycles: MWC is a good model for acetylcholine receptor-channels. *J. Physiol.* 590:93–98. https://doi.org/10.1113/jphysiol.2011.214684

Brown, A.M., A.G. Hope, J.J. Lambert, and J.A. Peters. 1998. Ion permeation and conduction in a human recombinant 5-HT3 receptor subunit (h5-HT3A). *J. Physiol.* 507:653–665. https://doi.org/10.1111/j.1469-7793.1998.653bs.x

Cao, L.Q., M.C. Montana, A.L. Germann, D.J. Shin, S. Chakrabarti, S. Mennerick, C.M. Yuede, D.F. Wozniak, A.S. Evers, and G. Akk. 2018. Enhanced GABAergic actions resulting from the coapplication of the steroid 3α-hydroxy-5α-pregnane-11,20-dione (alfaxalone) with propofol or diazepam. *Sci. Rep.* 8:10341. https://doi.org/10.1038/s41598-018-28754-7

Chang, Y., and D.S. Weiss. 1999. Allosteric activation mechanism of the alpha 1 beta 2 gamma 2 gamma-aminobutyric acid type A receptor revealed by mutation of the conserved M2 leucine. *Biophys. J.* 77:2542–2551. https://doi.org/10.1016/S0006-3495(99)77089-X

Colquhoun, D., and A.G. Hawkes. 1977. Relaxation and fluctuations of membrane currents that flow through drug-operated channels. *Proc. R. Soc. Lond. B.* 199:231–262. https://doi.org/10.1098/rspb.1977.0137

Colquhoun, D. 1973. The relationship between classical and cooperative models for drug action. *In* Symposium on Drug Receptors. H.P. Rang, editor. University Park Press, Baltimore, MD, USA. 149–182. https://doi.org/10.1007/978-1-349-00910-7_11

Eaton, M.M., L.Q. Cao, Z. Chen, N.P. Franks, A.S. Evers, and G. Akk. 2015. Mutational analysis of the putative high-affinity propofol binding site in human b3 homomeric GABAA receptors. *Mol. Pharmacol.* 88:736–745. https://doi.org/10.1124/mol.115.100347

Feng, H.J., Y. Jounaidi, M. Haburcak, X. Yang, and S.A. Forman. 2014. Etomidate produces similar allosteric modulation in α1β3δ and α1β3γ2L GABA(A) receptors. *Br. J. Pharmacol.* 171:789–798. https://doi.org/10.1111/bph.12507

Fletcher, G.H., and J.H. Steinbach. 1996. Ability of nondepolarizing neuromuscular blocking drugs to act as partial agonists at fetal and adult mouse muscle nicotinic receptors. *Mol. Pharmacol.* 49:938–947.

Forman, S.A. 2012. Monod-Wyman-Changeux allosteric mechanisms of action and the pharmacology of etomidate. *Curr. Opin. Anaesthesiol.* 25:411–418. https://doi.org/10.1097/ACO.0b013e328354feea

Germann, A.L., S.R. Pierce, A.B. Burbridge, J.H. Steinbach, and G. Akk. 2019a. Steady-state activation and modulation of the concatemeric α1β2γ2L $GABA_A$ receptor. *Mol. Pharmacol.* 96:320–329. https://doi.org/10.1124/mol.119.116913

Germann, A.L., J.H. Steinbach, and G. Akk. 2019b. Application of the Co-agonist concerted transition model to analysis of GABAA receptor properties. *Curr. Neuropharmacol.* 17:843–851. https://doi.org/10.2174/1570159X17666181206092418

Goldschen-Ohm, M.P., A. Haroldson, M.V. Jones, and R.A. Pearce. 2014. A nonequilibrium binary elements-based kinetic model for benzodiazepine regulation of GABAA receptors. *J. Gen. Physiol.* 144:27–39. https://doi.org/10.1085/jgp.201411183

Gottschald Chiodi, C., D.T. Baptista-Hon, W.N. Hunter, and T.G. Hales. 2019. Amino acid substitutions in the human homomeric β_3 $GABA_A$ receptor that enable activation by GABA. *J. Biol. Chem.* 294:2375–2385. https://doi.org/10.1074/jbc.RA118.006229

Goulding, E.H., G.R. Tibbs, and S.A. Siegelbaum. 1994. Molecular mechanism of cyclic-nucleotide-gated channel activation. *Nature.* 372:369–374. https://doi.org/10.1038/372369a0

Jones, M.V., Y. Sahara, J.A. Dzubay, and G.L. Westbrook. 1998. Defining affinity with the GABAA receptor. *J. Neurosci.* 18:8590–8604. https://doi.org/10.1523/JNEUROSCI.18-21-08590.1998

Karlin, A. 1967. On the application of "a plausible model" of allosteric proteins to the receptor for acetylcholine. *J. Theor. Biol.* 16:306–320. https://doi.org/10.1016/0022-5193(67)90011-2

Krogsgaard-Larsen, P., E. Falch, A. Schousboe, D.R. Curtis, and D. Lodge. 1980. Piperidine-4-sulphonic acid, a new specific GABA agonist. *J. Neurochem.* 34:756–759. https://doi.org/10.1111/j.1471-4159.1980.tb11211.x

Lema, G.M., and A. Auerbach. 2006. Modes and models of GABA(A) receptor gating. *J. Physiol.* 572:183–200. https://doi.org/10.1113/jphysiol.2005.099093

Li, S., and J. Zheng. 2024. How much does TRPV1 deviate from an ideal MWC-type protein? *Biophys. J.* 123:2136–2144. https://doi.org/10.1016/j.bpj.2024.04.005

Lingle, C.J. 2006. Empirical considerations regarding the use of ensemble-variance analysis of macroscopic currents. *J. Neurosci. Methods.* 158:121–132. https://doi.org/10.1016/j.jneumeth.2006.05.027

Masiulis, S., R. Desai, T. Uchański, I. Serna Martin, D. Laverty, D. Karia, T. Malinauskas, J. Zivanov, E. Pardon, A. Kotecha, et al. 2019. $GABA_A$ receptor signalling mechanisms revealed by structural pharmacology. *Nature*. 565:454–459. https://doi.org/10.1038/s41586-018-0832-5

Monod, J., J. Wyman, and J.P. Changeux. 1965. On the nature of allosteric transitions: A plausible model. *J. Mol. Biol.* 12:88–118. https://doi.org/10.1016/S0022-2836(65)80285-6

Mortensen, M., B. Frølund, A.T. Jørgensen, T. Liljefors, P. Krogsgaard-Larsen, and B. Ebert. 2002. Activity of novel 4-PIOL analogues at human alpha 1 beta 2 gamma 2S GABA(A) receptors--correlation with hydrophobicity. *Eur. J. Pharmacol.* 451:125–132. https://doi.org/10.1016/S0014-2999(02)02271-9

O'Shea, S.M., L.C. Wong, and N.L. Harrison. 2000. Propofol increases agonist efficacy at the GABA(A) receptor. *Brain Res.* 852:344–348. https://doi.org/10.1016/S0006-8993(99)02151-4

Pierce, S.R., S.Q. Xu, A.L. Germann, J.H. Steinbach, and G. Akk. 2024. Potentiation of the $GABA_AR$ reveals variable energetic contributions by etiocholanolone and propofol. *Biophys. J.* 123:1954–1967. https://doi.org/10.1016/j.bpj.2023.09.014

Rubin, M.M., and J.P. Changeux. 1966. On the nature of allosteric transitions: Implications of non-exclusive ligand binding. *J. Mol. Biol.* 21:265–274. https://doi.org/10.1016/0022-2836(66)90097-0

Ruesch, D., E. Neumann, H. Wulf, and S.A. Forman. 2012. An allosteric coagonist model for propofol effects on α1β2γ2L γ-aminobutyric acid type A receptors. *Anesthesiology*. 116:47–55. https://doi.org/10.1097/ALN.0b013e31823d0c36

Rüsch, D., H. Zhong, and S.A. Forman. 2004. Gating allosterism at a single class of etomidate sites on alpha1beta2gamma2L GABA A receptors accounts for both direct activation and agonist modulation. *J. Biol. Chem.* 279:20982–20992. https://doi.org/10.1074/jbc.M400472200

Saras, A., G. Gisselmann, A.K. Vogt-Eisele, K.S. Erlkamp, O. Kletke, H. Pusch, and H. Hatt. 2008. Histamine action on vertebrate GABAA receptors: Direct channel gating and potentiation of GABA responses. *J. Biol. Chem.* 283:10470–10475. https://doi.org/10.1074/jbc.M709993200

Sente, A., R. Desai, K. Naydenova, T. Malinauskas, Y. Jounaidi, J. Miehling, X. Zhou, S. Masiulis, S.W. Hardwick, D.Y. Chirgadze, et al. 2022. Differential assembly diversifies $GABA_A$ receptor structures and signalling. *Nature*. 604:190–194. https://doi.org/10.1038/s41586-022-04517-3

Sheridan, R.E., and H.A. Lester. 1977. Rates and equilibria at the acetylcholine receptor of electrophorus electroplaques: A study of neurally evoked postsynaptic currents and of voltage-jump relaxations. *J. Gen. Physiol.* 70:187–219. https://doi.org/10.1085/jgp.70.2.187

Shin, D.J., A.L. Germann, D.F. Covey, J.H. Steinbach, and G. Akk. 2019. Analysis of GABAA receptor activation by combinations of agonists acting at the same or distinct binding sites. *Mol. Pharmacol.* 95:70–81. https://doi.org/10.1124/mol.118.113464

Shin, D.J., A.L. Germann, J.H. Steinbach, and G. Akk. 2017. The actions of drug combinations on the GABAA receptor manifest as curvilinear isoboles of additivity. *Mol. Pharmacol.* 92:556–563. https://doi.org/10.1124/mol.117.109595

Sigworth, F.J. 1980. The variance of sodium current fluctuations at the node of Ranvier. *J. Physiol.* 307:97–129. https://doi.org/10.1113/jphysiol.1980.sp013426

Sine, S.M., and J.H. Steinbach. 1986. Activation of acetylcholine receptors on clonal mammalian BC3H-1 cells by low concentrations of agonist. *J. Physiol.* 373:129–162. https://doi.org/10.1113/jphysiol.1986.sp016039

Steinbach, J.H., and G. Akk. 2001. Modulation of GABA(A) receptor channel gating by pentobarbital. *J. Physiol.* 537:715–733. https://doi.org/10.1113/jphysiol.2001.012818

Steinbach, J.H., and G. Akk. 2019. Applying the monod-wyman-changeux allosteric activation model to pseudo-steady-state responses from $GABA_A$ receptors. *Mol. Pharmacol.* 95:106–119. https://doi.org/10.1124/mol.118.113787

Steinbach, J.H., and Q. Chen. 1995. Antagonist and partial agonist actions of d-tubocurarine at mammalian muscle acetylcholine receptors. *J. Neurosci.* 15:230–240. https://doi.org/10.1523/JNEUROSCI.15-01-00230.1995

Szabo, A., A. Nourmahnad, E. Halpin, and S.A. Forman. 2019. Monod-wyman-changeux allosteric shift analysis in mutant α1β3γ2L $GABA_A$ receptors indicates selectivity and crosstalk among intersubunit transmembrane anesthetic sites. *Mol. Pharmacol.* 95:408–417. https://doi.org/10.1124/mol.118.115048

Thompson, S.A., M.Z. Smith, P.B. Wingrove, P.J. Whiting, and K.A. Wafford. 1999. Mutation at the putative GABA(A) ion-channel gate reveals changes in allosteric modulation. *Br. J. Pharmacol.* 127:1349–1358. https://doi.org/10.1038/sj.bjp.0702687

Wotring, V.E., Y. Chang, and D.S. Weiss. 1999. Permeability and single channel conductance of human homomeric rho1 GABAC receptors. *J. Physiol.* 521:327–336. https://doi.org/10.1111/j.1469-7793.1999.00327.x

Zhang, Y., J. Chen, and A. Auerbach. 1995. Activation of recombinant mouse acetylcholine receptors by acetylcholine, carbamylcholine and tetramethylammonium. *J. Physiol.* 486:189–206. https://doi.org/10.1113/jphysiol.1995.sp020802

Zhou, M., A.G. Engel, and A. Auerbach. 1999. Serum choline activates mutant acetylcholine receptors that cause slow channel congenital myasthenic syndromes. *Proc. Natl. Acad. Sci. USA*. 96:10466–10471. https://doi.org/10.1073/pnas.96.18.10466

Zwart, R., and H.P. Vijverberg. 2000. Potentiation and inhibition of neuronal alpha4beta4 nicotinic acetylcholine receptors by choline. *Eur. J. Pharmacol.* 393:209–214. https://doi.org/10.1016/S0014-2999(00)00002-9